



HAL
open science

Sulfate Radical Technologies as Tertiary Treatment for the Removal of Emerging Contaminants from Wastewater

Monica Brienza, Ioannis Katsoyiannis

► **To cite this version:**

Monica Brienza, Ioannis Katsoyiannis. Sulfate Radical Technologies as Tertiary Treatment for the Removal of Emerging Contaminants from Wastewater. *Sustainability*, 2017, 9 (9), pp.1604. 10.3390/su9091604 . hal-02083501

HAL Id: hal-02083501

<https://hal.umontpellier.fr/hal-02083501>

Submitted on 18 Dec 2020

HAL is a multi-disciplinary open access archive for the deposit and dissemination of scientific research documents, whether they are published or not. The documents may come from teaching and research institutions in France or abroad, or from public or private research centers.

L'archive ouverte pluridisciplinaire **HAL**, est destinée au dépôt et à la diffusion de documents scientifiques de niveau recherche, publiés ou non, émanant des établissements d'enseignement et de recherche français ou étrangers, des laboratoires publics ou privés.



Distributed under a Creative Commons Attribution - NoDerivatives 4.0 International License

Article

Sulfate Radical Technologies as Tertiary Treatment for the Removal of Emerging Contaminants from Wastewater

Monica Brienza ^{1,2,*} and Ioannis A. Katsoyiannis ¹

¹ Department of Chemistry, Laboratory of Chemical and Environmental Technology, Aristotle University of Thessaloniki, 54124 Thessaloniki, Greece; katsogia@chem.auth.gr

² UMR HydroSciences 5569, Montpellier University, 15 Avenue Ch, 34093 Flahault, France

* Correspondence: monica.brienza@ird.fr; Tel.: +33-411-759-419

Received: 4 August 2017; Accepted: 24 August 2017; Published: 8 September 2017

Abstract: Water scarcity and water pollution is a worldwide problem and has driven research into eco-friendly and low-energy cost efficient remediation. The reuse of wastewater for non-potable purpose after proper treatment is the only sustainable solution to the problem. Advanced oxidation processes (AOP) based on the in-situ generation of hydroxyl radicals have been intensively investigated for this purpose as a treatment step to achieve wastewater reuse. The main degradation mechanism of AOPs is based on the reaction of hydroxyl radicals with dissolved organic matter. However, hydroxyl radicals follow unselective multi-step pathways, limiting their efficiency in complex environmental matrices. To overcome such limitations, AOP treatment, based on generation of sulfate radicals, has been developed and widely investigated. This current mini-review will cover the most recent developments regarding emerging contaminant removal, i.e., organic micropollutants, using sulfate radicals generated by active persulfate or peroxymonosulfate, with a focus on an application to wastewater effluents for possible wastewater reuse.

Keywords: sulphate radicals; AOP; oxidation; persulfate; peroxymonosulfate

1. Introduction

Water pollution by recalcitrant organic compounds is an increasingly important problem due to the continuous introduction of new chemicals into the environment. The recalcitrant organic compounds are well known as emerging contaminants—such as pharmaceuticals, pesticides, endocrine disruptors, and personal care products—and recent studies have showed that they are widely detected in water bodies [1–3]. Many emerging contaminants are toxic, biorefractory and difficult to be removed from wastewaters by the conventional treatment methods [4]. For this reason, it is necessary to improve the conventional wastewater treatment to enable the efficient removal of recalcitrant organics. Therefore, advanced oxidation processes are considered as an alternative or an additional step to conventional wastewater treatment plants, in order to enable the degradation of resistant organic compounds. The concept of “advanced oxidation processes” was defined by Glaze and co-workers in 1987 as the processes involving the in-situ generation of highly reactive species, able to attack and degrade organic substances [5].

Hydroxyl radicals are powerful, non-selective chemical oxidants that act rapidly with most organic compounds. Advanced oxidation processes give the possibility to produce hydroxyl radicals in situ by different possible processes. In water treatment, the most used are (i) Fenton oxidation; (ii) ozonation; (iii) photocatalysis and (iv) other methods. Researchers’ interest in AOPs began only around 1995 and continues today; in fact, there is an increase of the number of scientific papers in this topic, as is illustrated in the graph (Figure 1) based on the research results from Web of Science (May 2017).

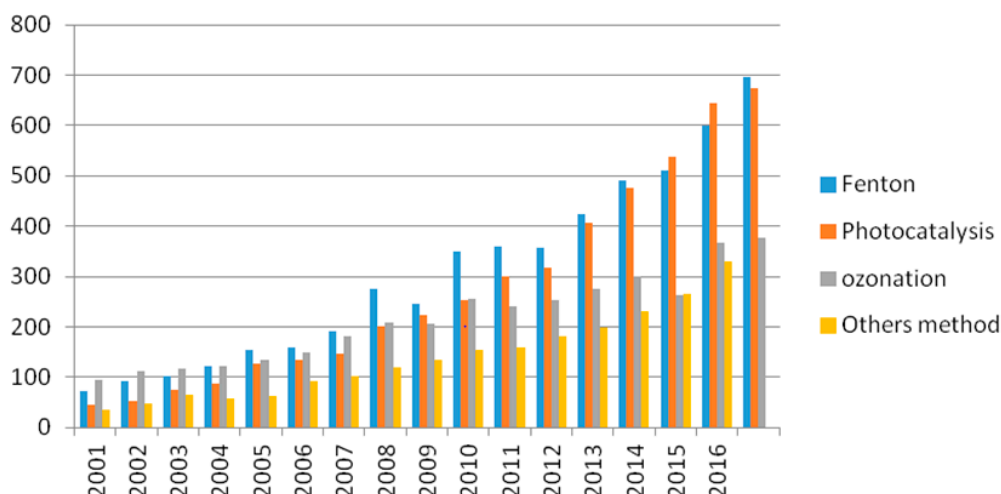


Figure 1. The accumulated numbers of scientific papers on advanced oxidation processes (AOP) to water treatment. The data are based on search results from Web of Science (May 2017).

Briefly, the main processes used in wastewater treatment are the following:

(i) The Fenton and/or photo Fenton processes: Fenton H.J.H. in the 1890s discovered the reaction of polycarboxylic acid with hydrogen peroxide (H_2O_2), and observed that a strong promotion took place in the presence of ferrous ions (Fe^{2+}). The Fenton process, or dark Fenton, involves the use of an oxidant, generally H_2O_2 , and a catalyst, usually iron in the form of ferrous ions. The generation of hydroxyl radicals are formed by the oxidation of Fe^{2+} . The main applicative limits are that this process occurs in the acid medium, and that iron removal is required.

The photo Fenton process involves irradiation with sunlight or an artificial light source. The presence of light improves the efficiency of the treatment thanks to the photoreduction of the Fe^{3+} to Fe^{2+} , which results in additional generation of hydroxyl radicals. This process requires additional cost for the UV irradiation.

(ii) Ozonation: Ozone is a powerful oxidizing agent, which is able to participate in a great number of reactions with organic and inorganic compounds. Since the beginning of the century, it has been used as disinfectant, but only in the last decades has it acquired notoriety in wastewater treatment. In the absence of light, ozone can react directly with organic compounds through a slow and selective reaction, or through a fast and non-selective reaction through the formation of hydroxyl radicals. The presence of UV light can generate additional hydroxyl radicals due to the photolysis of O_3 , increasing the efficiency.

The main disadvantages are the low solubility of O_3 in water, the formation of hazardous by-products, in particular, bromate formation, and the elevated energy costs [6].

Unfortunately, there are many literature reports concerning industrial wastewater treatment by AOPs, especially about textile wastewater, but most of them are not oriented on the industrial application. In this scenario, [7] demonstrated that some of those oxidative processes can be suitable for industrial application. The research group reported that, based on the experimental result and cost evaluation, the use of ozone or ozone with a very low concentration of hydrogen peroxide (0.005 M) can be recommended to the textile industry. In contrast to the O_3/UV treatment, the investment and operating cost are much higher than ozonation itself. Therefore, the main application of ozonation is for disinfection in wastewater treatment plants for drinking water.

(iii) Photocatalysis: This AOP is based on the use of a semiconductor as catalyst and a light source. Several semiconductors have been used in this field, but titanium dioxide (TiO_2) proved to be the most appropriate due its characteristics such as high photoactivity, chemical inertness, non-toxicity, and low cost [8]. The initiating procedure of the photocatalytic reaction is the adsorption of the radiation with the formation of holes (h^+) in the valence band and electrons (e^-) in the conduction band.

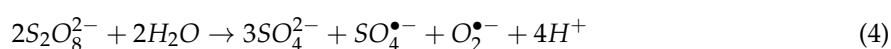
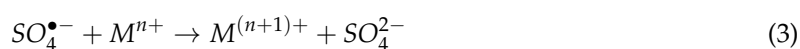
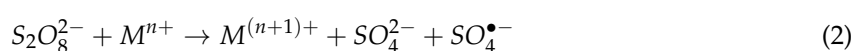
(iv) There are other methods among AOPs; however these are non-photochemical, such as electro-Fenton and wet air oxidation. There are two main types of electro-Fenton. In cathodic processes, iron is added as Fe^{2+} or Fe^{3+} salt. The source of H_2O_2 may be either via direct H_2O_2 addition or produced by reduction of oxygen at the cathode. In the anodic process, the source of iron is a sacrificial iron anode. This treatment requires a high iron concentration and elevated costs.

The wet air oxidation is defined as the oxidation of substances in aqueous solution by means of oxygen or air at elevated temperature and pressure; for this reason, it has a high operational cost.

Hydroxyl radicals proceed through unselective multi-step pathways which limit its efficiency in complex environmental matrices; for example, waters which contain high concentrations of the main hydroxyl radical scavengers in wastewater, i.e., dissolved organic matter (DOM) and carbonate/bicarbonate anions [9]. This increases the overall scavenging rate of waters to be treated [6]. To overcome this limitation, novel more selective methods, producing reactive radicals, were developed. Use of sulfate radical ($\text{SO}_4^{\bullet-}$) technologies is a recent example. In fact, Ahmed et al. [10] reported that sulfate radicals attack through the one electron oxidation mechanism, limiting the scavenging effect of DOM and inorganic ions [10,11].

Few works have reported the comparison between sulphate radical (SR) and hydroxyl radical (HR) technologies. Table 1 compares the advantages and disadvantages of various AOPs, while Table 2 compares the kinetic rates of HR and SR. [12] investigated the kinetic rate of six organic compounds under SR and HR oxidation. The SR technology was always 10 times faster than HR systems; except for carbamazepine, for which the kinetic constant was less than seven-fold higher than with HO. Other works reported that HR systems were more efficient than sulphate radicals on ibuprofen or levofloxacin abatement [13–15].

Sulfate radicals ($\text{SO}_4^{\bullet-}$) serve as powerful oxidants with a standard redox potential of 2.6 V, comparable to the standard potential of HO^{\bullet} (2.8 V) [16] that can be generated in situ by the activation of the most common precursors, namely potassium persulfate (PS) or peroxymonosulfate salt (PMS), by a variety of approaches such as photolysis, radiation and thermal activation (Equations (1)–(8)). Between these methods, the addition of transition metals is recognized to be a viable way to enact the homogenous activation of (persulfate/peroxymonosulfate) PS/PMS [17].



Generally, peroxymonosulfate is activated to produce both radicals, sulfate and hydroxyl, when its peroxide bond (-O-O-) is homolitically cleaved, as reported in the following equations (Equations (6)–(8)) [18].

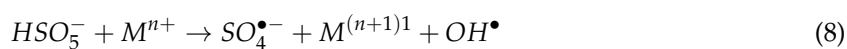
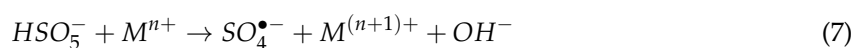


Table 1. Main advantages and disadvantages of various Advanced Oxidation Processes.

| AOP | Advantages | Disadvantages |
|---|---|---|
| Fenton's Reaction | <ul style="list-style-type: none"> • Able to degrade soluble and insoluble dyes in industrial effluents • No potential formation of bromated by product | <ul style="list-style-type: none"> • Iron sludge generation due to combined flocculation of the reagent and the organic compounds • Low pH (<2.5) is required to keep iron in solution • pH adjustment will increase operating cost |
| TiO ₂ catalyzed UV oxidation | <ul style="list-style-type: none"> • No potential formation of bromated by product • Recycling of the catalysts • Performance also at higher wavelengths and under solar irradiation | <ul style="list-style-type: none"> • No full-scale application exists • If the catalyst is added as a slurry, separation step is required • Adapted and optimum concentration of catalyst required a rigorous studies |
| H ₂ O ₂ /O ₃ | <ul style="list-style-type: none"> • Formation of strong non-selective hydroxyl radicals that are able to break down the conjugated double bond • Ozone can be used in its gaseous state and consequently does not raise the volume of wastewater • No sludge generation | <ul style="list-style-type: none"> • Low rate of degradation as equated to the AOP processes due to less production of hydroxyl radicals • Ozone may form toxic by-products • High cost • Requires treatment of excess H₂O₂ due to potential for microbial growth |
| O ₃ /UV | <ul style="list-style-type: none"> • More efficient than O₃ or UV alone • Disinfectant • For equal oxidant concentration, more efficient at generating hydroxyl radical than H₂O₂/UV | <ul style="list-style-type: none"> • Potential bromated by product • UV light penetration can be obstructed by turbidity • Compounds such as nitrate can interfere with the absorbance of UV light • Energy and cost intensive processes |
| H ₂ O ₂ /UV | <ul style="list-style-type: none"> • No potential formation of bromated compounds • Full scale drinking water treatment system exists | <ul style="list-style-type: none"> • Potential bromated by product • UV light penetration can be obstructed by turbidity • Compounds such as nitrate can interfere with absorbance of UV light |
| Sonication | <ul style="list-style-type: none"> • Less heat transfer relative to UV system • No bromated formation if O₃ is not added | <ul style="list-style-type: none"> • No full scale application exists • Oxidant may be needed to improve the efficiency of the treatment, thereby increasing cost |

Table 2. Comparison between sulphate radical (SR) and hydroxyl radicals (HR) technologies.

| Targeted Compound | <i>k</i> SR | <i>k</i> HR | Reference |
|-------------------|---|---|-----------|
| Sulfamethoxazole | $54.12 \pm 0.1 \times 10^{-2} \text{ min}^{-1}$ | $3.12 \pm 0.02 \times 10^{-2} \text{ min}^{-1}$ | [12] |
| Bifenthrin | $28.65 \pm 0.06 \times 10^{-2} \text{ min}^{-1}$ | $1.65 \pm 0.08 \times 10^{-2} \text{ min}^{-1}$ | |
| Mesotrione | $21.32 \pm 0.08 \times 10^{-2} \text{ min}^{-1}$ | $1.45 \pm 0.07 \times 10^{-2} \text{ min}^{-1}$ | |
| Carbamazepine | $18.69 \pm 0.03 \times 10^{-2} \text{ min}^{-1}$ | $2.96 \pm 0.01 \times 10^{-2} \text{ min}^{-1}$ | |
| Diclofenac | $58.19 \pm 0.4 \times 10^{-2} \text{ min}^{-1}$ | $3.65 \pm 0.06 \times 10^{-2} \text{ min}^{-1}$ | |
| Ibuprofen | $1.66 \pm 0.12 \times 10^9 \text{ M}^{-1} \text{ s}^{-1}$ | $3.43 \pm 0.06 \times 10^9 \text{ M}^{-1} \text{ s}^{-1}$ | [13] |
| | $1.32 \times 10^9 \text{ M}^{-1} \text{ s}^{-1}$ | $5.57 \times 10^9 \text{ M}^{-1} \text{ s}^{-1}$ | [14] |
| Levofloxacin | $0.93 \pm 0.02 \times 10^{-2} \text{ min}^{-1}$ | $20.81 \pm 0.7 \times 10^{-2} \text{ min}^{-1}$ | [15] |

Advanced oxidation processes based on sulfate radical generation have proved to be effective in degrading a wide range of recalcitrant micro contaminants in aqueous solutions, including hormones [19], pharmaceuticals [1,20], herbicides [12] and the decontamination of pool water [21].

Therefore, this technology is considered as a promising method for tertiary wastewater treatment because it is able to produce treated effluent that can be reused for agriculture or industrial activities. Table 1 summarizes the advantages and disadvantages of the AOP methods used in the wastewater treatment. Based on this information, the aim of this review study is to report the fundamentals and the recent advances of the application of sulphate radicals in wastewater treatment technologies, with the

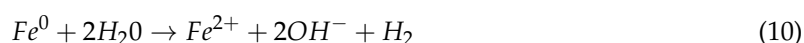
purpose of providing insight towards the application of such technologies for efficient water reuse for applications in water-scarce regions and vulnerable communities.

2. Sulfate Radicals for the Treatment of Wastewater

Different advanced oxidation technologies have been studied and applied for the treatment of domestic and various industrial (e.g., winery, textile, paper, etc.) wastewaters [22,23]. The efficiency of the treatment depends on many parameters, such as the type of wastewater, chemical properties of contaminants, pH of water, concentrations of scavengers, operating conditions. In this article, we summarized the advanced oxidation processes based on sulfate radicals for the treatment of a domestic wastewater effluent. Wastewater effluent is considered the most promising source for production of recycled water [24]. Reused wastewater should be free of toxic or xenobiotic substances such as pesticides, pharmaceuticals, and endocrine disrupting compounds [25].

3. Ferrous Activation Systems

One of the most popular advanced oxidation processes are Fenton-like processes. The Fenton-like reaction can be performed through the activation of PS or PMS, as an oxidant, and the pair of Fe^{2+}/Fe^{3+} , as a catalyst, according to Equations (2), (3), (7) and (8). The generation of sulfate radicals through Fe^{2+} has a great potential for the degradation of various recalcitrant compounds such as aniline, pesticides, chlorophenols and azo dyes [26,27] or for the treatment of stabilized leachates [28]. Rastogi and co-workers [29] have shown that sulfate radicals generated from activation of peroxymonosulfate by $Fe(II)$ were able to destroy polychlorinated biphenyls (PCBs) in aqueous and sediment systems. This system had been used in situ for chemical oxidation in wastewater treatment as reported in different studies [30,31]. This treatment has some limitations such as the fast conversion of $Fe(II)$ in $Fe(III)$ and acidic pH of the solution [32]. To overcome this applicative limit, various studies were developed using different sources of iron. Zero valent iron (ZVI) was deeply researched as an alternative source of $Fe(II)$ which is able to activate persulfate. In the system using ZVI/PS, $Fe(II)$ is produced by corrosion under oxic/anoxic condition and/or oxidation by PS, resulting in the release of Fe^{2+} , which can activate persulfate to generate sulphate radicals (Equations (9)–(12)) [33]:



SR generation by the reduction of zero valent iron (ZVI) has been recently investigated and considered as good strategy for the removal of recalcitrant compounds such as polyvinyl alcohol (PAV) [34], pesticides such as alachlor [35], herbicides such as bentazon [36], volatile gas as methyl mercaptan [37] and 1–4 dioxane [38]. The use of this source of iron has the advantages of low cost and easy operation; but it has a tendency to agglomerate due to the high surface energy and intrinsic magnetic interaction [39]. To improve the efficiency and decrease the aggregation of ZVI particles, recent research has investigated the encapsulation on a catalyst. Different kinds of materials have been investigated such as mesoporous silica microsphere, kaolinite, carbon [40–42], all of which have shown a great performance in transforming persistent pollutants in less toxic products.

These results were also confirmed by studies that have showed that modified zero valent iron showed a greater performance in the removal of various pollutants than non-modified ZVI [39,43]. In more recent studies, Diao and co-workers [44] reported the efficiency of bentonite-supported nanoscale zero-valent iron as a catalyst able to activate persulfate, and produce SR, which was confirmed from a positive correlation between persulfate decomposition and dissolved $Fe(II)$.

This heterogeneous treatment was able to remove, simultaneously, heavy metals such as chromate (Cr(VI)) and organic pollutants such as phenol from contaminated aqueous solutions.

Additionally, several studies have been reported in literature to use different organic chelating agents (e.g., citric acid, ethylenediaminetetraacetic acid (EDTA)) which were able to activate the persulfate system and to increase the contaminant degradation effectiveness. Liang and co-workers reported that the addition of citric acid in Fe(II) [45] in persulfate system improved the trichloroethylene (TCE) degradation by stabilizing Fe(III) and preventing its precipitation as iron hydroxide/iron oxide. Other studies investigated the development of SR using EDTA to remove TCE from aqueous solution [46]. This study showed that the presence of Fe(III) and EDTA alone and in combination did not cause any significant increase in persulfate activation. The presence of TCE in the EDTA/Fe(III) activated persulfate system significantly enhanced persulfate activation, and the application of an EDTA/Fe(III) mixture was successfully applied for the degradation of TCE in solution at various pH conditions. Furthermore, Dulova and co-workers [47] confirmed that the addition of citric acid as a chelating iron agent improved the naproxen destruction by the oxidation process. The highest performance was obtained when the oxidant agent used was persulfate instead of hydrogen peroxide.

In Fenton or Fenton-like processes, the slow regeneration of Fe(II) and production of ferric hydroxide sludge restrict its usage, because of passivation and loss of activity [48]. Therefore, an improvement of this process implies the application of irradiation, which greatly improves the photo-reduction of Fe(III)-complex in Fe(II) (Equation (13)).



The efficiency of the Fenton process can be improved through the addition of radiation (sunlight or artificial sources of UV radiation). The photochemical reduction of Fe(III) is able to generate additional hydroxyl radicals, so the efficiency of the processes increases [49,50]. The artificial generation of photons required for the detoxification of polluted water is the most important source of costs during the operating of photocatalytic wastewater treatment plants. In fact, the photo-Fenton treatment developed under solar irradiation as a UV-Vis photon source is a potentially low-cost technique [51,52]. Recent findings demonstrated the ability of photo-Fenton treatment to remove micro-pollutants at relatively low concentrations (ng/L-µg/L) [53,54]. Recently, Malato's group [55] studied the solar photo-Fenton optimization for the treatment of municipal wastewater effluents. The important outcome of this study was that iron concentration, temperature and their interaction are the most important parameters necessary to remove over 95% of the organic contaminant targets. Another important observation was that a high concentration of hydrogen peroxide (up to 70 mg/L) decreased the processes efficiency [55].

Solar photo-Fenton is not the only treatment investigated in this topic; solar photocatalysis using titanium dioxide (TiO₂) have also been investigated. It has also reported [56] that solar TiO₂ technologies were able to eliminate toxicity and completely mineralize recalcitrant compounds present in raw oil sand process-affected water (OSPW). Malato et co-workers [57] developed an interesting review on the use of sunlight to produce the hydroxyl radicals by TiO₂ and encourage further relevant research with possible applications in industrial processes.

Titanium dioxide is not only the catalyst used in solar photocatalysis technologies. Dhatshanamurthi and co-workers [58] developed an interesting study and dealt with an efficient pilot scale solar for the treatment of dye industry effluent based on the generation in situ of hydroxyl radicals. The solar treatment was carried out using prepared nano-ZnO, commercial ZnO and titanium dioxide P25 (TiO₂-P25). The catalyst made on thin film was stable and reusable for several cycles, so this make the solar treatment processes suitable for industrial effluent.

Despite the growing interest in AOPs, there are very few large-scale applications of solar-activated AOPs based on the generation of sulfate radicals. Among them, Brienza and co-workers [19] demonstrated that sulfate radical-based homogenous advanced oxidation technologies involving peroxymonosulfate as an oxidant and ferrous iron (Fe(II)) as a catalyst had better kinetic results

when compared to solar photo-Fenton (UV-Vis/H₂O₂/Fe(II)) and heterogeneous photocatalysis using titanium dioxide (UV-Vis/TiO₂) for the removal of 17β-estradiol in wastewater. Little attention has been paid to advanced oxidation processes applied directly to wastewater effluents. Brienza and co-workers [1] reported that solar advanced oxidation processes showed that emerging contaminants at low concentrations can be successfully degraded. The aim of this work was to apply the solar AOP based on sulfate (SR) or hydroxyl radical (HR) on wastewater effluents. Both technologies (SR or HR) were able to transform part of the 53 micro-pollutants detected in the effluents. The results were very promising and further research is under way.

The full-scale treatment developed by solar-enhanced Fenton-like processes involving persulfate and ferrous ion was able to cause a complete degradation of atrazine and a 20% reduction in total organic carbon (TOC) content observed after 30 min of the treatment, as reported by Khandarkhaeva et co-workers [59]. The relevance of this study was the demonstration that the high efficiency of the solar processes was due to the additional formation of hydroxyl and sulfate radicals generating from the photo-reduction of Fe_{aq}³⁺, FeOH²⁺ and Fe₂(OH)₂⁴⁺ and decomposition of S₂O₈²⁻. Therefore, in this scenario, iron was acting not only as catalyst but also as photo-sensitizer [59].

Lin and Wu [60] investigated at a large scale the degradation of ciprofloxacin by UV/S₂O₈²⁻. The relevance of this study was that the degradation of the target compound increased with persulfate concentrations until the excess of it started to inhibit the processes.

4. Non-Ferrous Activation Systems

Iron is not the only transition metal investigated in this field. In fact, the cobalt used for activation of peroxymonosulfate (Co²⁺/PMS) was studied [61]. Later studies showed that Co²⁺/PMS systems were found to show the best performance at neutral pH and with a lower dosage of PMS [62,63]. Moreover, Zhang et al. [63] reported the activation of persulfate by nano-Co₃O₄ for orange G degradation, and it was reported that the nanoparticles were stable, with a slight decline in the catalytic ability due to the oxidation of surface Co(II) to Co(III). The nanoparticles were able to activate potassium persulfate (PS), peroxymonosulfate (PMS) and sodium persulfate (NaPs). The efficiency in terms of time need to remove orange G followed the order nano-Co₃O₄/PMS > nano-Co₃O₄/PS > nano-Co₃O₄/NaPS.

The main disadvantage observed was the Co leaching during the catalytic processes, which limits its use in environmental applications. In order to reduce this undesirable effects, Co₃O₄ has been decorated on various supports including cobalt ferrite [64], silica support [65], graphene oxide [66]. The supported catalyst of cobalt, generally, showed better catalytic activity, reducing Co leaching, and better separation of the catalyst from the treated water. However, this did not eliminate the Co leaching problem.

Other transition metals used for the activation of persulfate or peroxymonosulfate were investigated. Saputra et al. [67] used various types of manganese oxides (MnO, MnO₂, Mn₂O₃ and Mn₃O₄) for activation of PMS and studied phenol removal. They found that the catalytic activity of Mn oxides was dependent on the chemical states of Mn. Mn₂O₃ was the most effective among the Mn oxide tested.

Liu et al. [68] reported a comparison study of propachlor degradation by persulfate activation using two metal ions such as Cu(II) and Fe(II), respectively. Both metals ions were able to activate persulfate and degradate the target molecules. The kinetic behaviour was different, in fact, when Fe(II) was used; the degradation was initially quite fast and afterwards slower, due to the rapid depletion of Fe(II) by the generated sulfate radicals. Copper ion activated persulfate was proven to achieve steady and efficient degradation of propachlor.

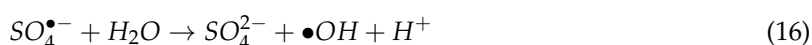
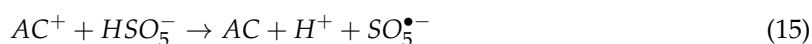
Recently, for the first time, Fang and co-workers [69] demonstrated that vanadium species are able to activate persulfate for the degradation of contaminants. The most efficient system for the degradation of target molecules (2,4,4'-trichlorobiphenyl [PCB28]) was V₂O₃/PS; VO₂ and V₂O₅ also can activate PS, but the degradation of PCB28 was significantly lower. Vanadium is a natural element,

widely-distributed particularly in soil, so the natural occurrence is able to activate persulfate and can provide the possibility to apply this technique for the purification of wastewater.

5. Non-Metal Carbon Catalysts

Recently, several studies investigated the ability of non-metal carbon catalysts as a potential solution to the metal leaching problem, and to constitute metal-free environmental catalysts [70,71]. The most studied was activated carbon (AC) due to its relatively low cost and the wide applications in the water/wastewater treatment industry. Activated carbon shows catalytic activity due to its oxygen functional group on the surface, which favors electron-transfer. Kimura et al. [72] and Liang et al. [46] reported the ability of activated carbon to activate hydrogen peroxide and persulfate, respectively.

Different forms of activated carbon have been intensely investigated as material able to show synergistic effects both as adsorbent and catalyst. The particle size plays an important role on activated carbon activity, because its performance as a PMS activator depends of the density of the surface. Saputra et al. (2013), [67] demonstrated that powdered activated carbon (PAC) was much more effective than granular activated carbon (GAC) and proposed the following reaction mechanisms:



Several studies showed the potential of activated carbon to activate oxidant agents able to destroy several recalcitrant organic compounds. Muhammed and co-workers [73] reported the comparison of catalyst efficiency between RuO₂/AC and RuO₂/ZSM5. Both catalysts were able to activate PMS and able to destroy phenol in aqueous solutions, but activated carbon had better performance. Yang et al. [74] proved that, in a carbon filter/PMS system, the catalytic oxidation made a major contribution to total acid orange 7 removal rather than adsorption. Similar results were obtained by Zhang et al. [75], where the decolorization of acid orange 7 solution was accomplished using granular activated carbon/peroxymonosulfate system. Unfortunately, the catalyst capacity of AC is not durable, as its adsorption capacity decreases with repeated use [75]. To overcome these limitations, post-treatment processes such as heating or chemical activation are required, increasing the cost of the treatment.

6. Graphenes as Activation Medium for PMS

Activated carbon is not the only carbon catalyst investigated in water/wastewater treatment. Recently, great attention has been given to the use of graphene and its derivatives. Wang's group investigated intensively on this topic, developing research on a wide variety of carbon allotropes in different molecular dimensions, such as reduced graphene oxide (rGO), single walled carbon nanotubes (SWCNTs), mesoporous carbon (CMK-8), nanodiamonds, graphitic carbon nitride (g-C₃N₄), and fullerene (C₆₀) [70]. At first, they discovered that rGO developed by chemically synthesized graphene oxide by the one-pot thermal method was found to be effective in the metal-free activation of PMS to generate reactive radicals for the oxidation of methylene blue [76]. Successively, they showed that the adsorption capacity of nanocarbons was related to the structure; in fact, the 3D structure had a bigger porosity and larger specific area, thus giving higher phenol adsorption. Additionally, its catalytic activity for the activation of PS was tested on phenol degradation, and it was found that SWCNTs, CMK-8, and rGO-900 presented outstanding performances for PS activation, providing complete phenol degradation in 90, 45 and 30 min, accordingly [70].

The activation of persulfate or peroxymonosulfate on carbon based catalysts is not fully understood. It has been reported that the activation mechanism is not only by radicals but also a non-radical pathway bridging the formation of both OH• and SO₄^{•-} radicals using N-doped single

walled carbon nanotubes for PMS activation [70]. The occurrence of radical and non-radical pathways depends on the type of carbon structure [77]. The non-metal carbon catalyst/oxidant agent system can be an alternative treatment for wastewater effluents. More investigations should be performed because this is a very promising idea, and to date, no large-scale applications or pilot plants have been carried out. It should be observed whether this system can also be efficient in real effluent, rich in normal organic matter, which normally are able to scavenge the radical species.

7. Hybrid Advanced Oxidation Processes Based on Sulfate Radicals

Hybrid advanced oxidation processes based on coupling of either UV-Vis or microwave irradiation or ultrasonic (US) with heterogeneous catalyst/PMS have been investigated to improve the oxidation efficiency. Under UV-Vis irradiation, one of the catalysts studied is titanium dioxide (TiO_2). Chen et al. [78] reported that peroxymonosulfate was able to accelerate the TiO_2 photocatalyst of acid orange 7 under visible light. The performance of this system was better than UV-Vis/ TiO_2 /PS and UV-Vis/ TiO_2 / H_2O_2 . Furthermore, the presence of humic acid has positive effect on degradation of acid orange 7 under UV-Vis/ TiO_2 /PMS. Similar results were reported by Kuriechen et co-workers [79], where the photodegradation rate of textile dyes such as reactive red 180 (RR180) increased by 10-fold adding peroxymonosulfate (e.g., oxone) in the UV-Vis/ TiO_2 system. Other hybrid systems coupling microwave irradiation with catalyst/PMS have been reported to have a positive effect on P-nitrophenol removal (PNP) [80]. In fact, the microwave irradiation accelerated the processes and achieved almost 98% degradation of PNP in 2 min using PMS/ MnFe_2O_4 /MW. The main advantage of microwave irradiation is that the temperature of aqueous solution increases and can create hotspots on the catalyst surface. Therefore, in such cases, it is really important to know the stability of the used catalysts. Many parameters influence the efficiency of this treatment such as (i) the right quantity of the catalyst; (ii) the quantity of the oxidant agent; (iii) pH of the solution; (iv) the photon flux. Table 3 summarizes the main characteristics of metal catalysts used in the production of sulphate radicals.

Table 3. Comparison of performance of metal catalysts ($\text{SO}_4^{\bullet-}$).

| Target Pollutant | | Performance | Reference |
|--|-------------------------------|---|-----------|
| Metal Catalyst | | | |
| Fe(II) | Aniline | <ul style="list-style-type: none"> >90% of 33 μM aniline removed in 200 s with 1.83 mmol L^{-1}, PS 0.1 mmol L^{-1}, pH 7 | [26] |
| | Atrazine and TOC | <ul style="list-style-type: none"> UV/PMS/Fe(II) was efficient to the degradation of atrazine at pH 3; UV/PS/Fe(II) was efficient in terms of TOC removal and degradation of atrazine at pH 5.8 | [27] |
| Fe(III)/chelating agent | Iopamidol | <ul style="list-style-type: none"> [IPM] = 20 μM, [PS]₀ = 0.2 mM, [Fe(II) or Fe(III)]₀ = 10 μM, [complexing agent]₀ = 10 μM, pH₀ = 7 Galic acid outperformed EDTA, Ethylenediamine-<i>N,N'</i>-disuccinic acid (EDDS) and CA for the activation of PS/Fe(III) The degradation of IPM by GA/PS/Fe(III) increased about 10.2 and 7 times by PS/Fe(III) and PS/Fe(II), respectively OH played an important role than SO_4^{-2} in IPD degradation by GA/PS/Fe(III) | [33] |
| ZVI | Bisphenol and phosphate | <ul style="list-style-type: none"> ZVI/PS was able to remove simultaneously BPA and phosphate [BPA] = 22 μM, [PS] = 1 mM, [ZVI]₀ = 0.5 g L^{-1}, [P]₀ = 5 mg L^{-1}, pH₀ = 6 in wastewater ZVI/PS removed 74% BPA and 91% phosphate | [81] |
| | Dibutyl phthalate | <ul style="list-style-type: none"> Total degradation of DBP by ZVI/PS Active species at pH 3 and pH 7 were $\text{SO}_4^{\bullet-}$ and $\bullet\text{OH}$ OH was the major oxidant at pH 11 | [82] |
| Cobalt | DDT | <ul style="list-style-type: none"> [PMS] = 2.0 mM, [Co²⁺] = 20 μM, pH = 3, DDT = 1 mg L^{-1}, T = 30 °C in 120 min total degradation (100%) of DDT | [83] |
| Co-based metal organic frameworks (MOFs) | Dibutyl phthalate | <ul style="list-style-type: none"> Co-BTC was synthesized by two solvothermal methods (A and B) Co-BTC(A) shown great capability to activate peroxymonosulfate 100% degradation of DBP in 30 min After three run, the decline of DBP degradation was observed | [84] |
| Copper oxidate | <i>p</i> -chloroaniline [PCA] | <ul style="list-style-type: none"> [PCA]₀ = 0.5 mM, [PS]₀ = 2.5 mM, [copper oxidate]₀ = 0.5 g L^{-1}, pH = 7 total degradation of PCA in 300 min Optimal molar ratio PS/PCA was 5/1 PCA degradation was better at pH 7 than acid and alkaline condition | [85] |
| Copper ion | Propachlor | <ul style="list-style-type: none"> Degradation of propachlor in situ by Cu²⁺ activated persulfate was higher than Fe²⁺ activation The activation using Cu²⁺ was enhanced at 55 °C the activation | [68] |
| Fe/Cu | <i>p</i> -nitrophenol (PNP) | <ul style="list-style-type: none"> TMLCu of 0.173 g Cu/g Fe, mFe/Cu of 30 g L^{-1}, PS of 12.5 mM, pH of 3.6, T of 25 °C, 98.4% of PNP at initial concentration 500 mg L^{-1} was remove after only 3 min PS can enhance the reactivity of Cu by rapid carrion of iron surface | [86] |

Table 3. Cont.

| | Target Pollutant | Performance | Reference |
|--|---------------------------------|---|-----------|
| Manganite | Phenol | <ul style="list-style-type: none"> • α-Mn₂O₃, Mn₃O₄ and γ-MnOOH used for activate persulfate • Only γ-MnOOH was to able to activate PS and remove 80% of phenol in 360 min • The system was pH dependent, in fact at pH 11, the phenol oxidation is more complete than at pH 7 and 3 | [87] |
| Vanadium | 2,4,4-trichlorobiphenyl [PCB28] | <ul style="list-style-type: none"> • V₂O₃/PS was efficient catalyst for activate persulfate and remove PCB28 better than VO₂ and V₂O₅ • V₂O₃/PS was performance at neutral pH 7.49 • Loading of vanadium was less than the natural quantity of vanadium in the soil (90 mg Kg⁻¹) | [69] |
| Zn ⁰ | Methyl orange (MO) | <ul style="list-style-type: none"> • Optimal condition:[PS] = 71 mg L⁻¹, [Zn⁰] = 1.3 g L⁻¹, [MO] = 98 mg L⁻¹, pH = 5, T = 25 °C • 3 h was the duration of the treatment • Efficiency at the end of the treatment: 90% MO removal, decrease 80% of COD and 58% of TOC | [39] |
| Metallic glass (Fe _{73.5} Si _{13.5} B ₉ Cu ₁ Nb ₃) | Malachite green (MG) | <ul style="list-style-type: none"> • MG (20 ppm) was completely degraded within 30 min by activated persulfate (1.00 mmol L⁻¹) through Fe_{73.5}Si_{13.5}B₉Cu₁Nb₃, ribbon dosage (0.5 g L⁻¹) under UV-Vis irradiation (7.7 μW cm⁻²) | [88] |
| Metal-free catalyst | | | |
| Bicarbonate | Acetaminophen | <ul style="list-style-type: none"> • [HCO₃⁻] = 25 mM, [acetaminophen] = 10 μM, [PS] = 5 mM, pH = 8.3, T = 25 °C, 50% of acetaminophen was removed after 8 h of treatment • Activation of PS by bicarbonate forms HCO₄⁻ which gives rise to O₂^{•-} and ¹O₂ subsequently • Degradation due to the reaction between HCO₄⁻ with acetaminophen via single-electron oxidation mechanism | [89] |
| Powder activated carbon (PAC) | Phenol | <ul style="list-style-type: none"> • Complete phenol [25 mg L⁻¹] remove in 15 min using [PAC] = 0.2 g L⁻¹; [PMS] = 6.5 mmol L⁻¹ at 25 °C • PAC exhibited higher activity than granular activated carbon and hight activity in PMS activation | [67] |
| S-doped activated carbon (ACS) | 4-chlorophenol (4CP) | <ul style="list-style-type: none"> • ACS degraded 100% 4CP, 65.3% COD in 170 min at 25 °C, ACS dosage of 0.1 g L⁻¹, PS/4CP molar ratio 24/1, initial pH at 4.4 • SO₄^{•-} was the dominant active specie during this treatment | [90] |
| Carbon nanotubes (CNTs) | Phenol | <ul style="list-style-type: none"> • Single-CNTs and multi-walled CNTs were used for activated persulfate • Single-CNTs exhibited higher activity than MWCNT • Activation was via non radical mechanisms | [91] |
| Nitrogen-CNT | Phenol | <ul style="list-style-type: none"> • Nitrogen doping on carbon nanotube enhances the catalytic activity of 7.8 fold • NCNT was able to activate PMS, any activation was observed on PS • CNT-C = N + HSO₅⁻ → CNT-C-N* + SO₄^{•-} + OH⁻ | [92] |

Table 3. Cont.

| Target Pollutant | | Performance | Reference |
|--|---|--|-----------|
| Nitrogen doped Reduced Graphene Oxide (N-rGO) | sulfachloropyridazine (SCP) | <ul style="list-style-type: none"> N-rGO can activate PS and remove completely SCP N-rGO catalyst can be reuse First run: 100%; second run: 82% and third run: 58% SCP removal, respectively N-rGO/PS is not pH dependent | [93] |
| Annealed Nanodiamonds (ANDs) | Phenol, catechol, benzoic acid, sulfachloropyridazine, methylene blue | <ul style="list-style-type: none"> ANDs was able to activate persulfate to generate sulfate and hydroxyl radicals Organic pollutants were removed in few minutes High reusability of the catalyst | [77] |
| Hybrid AOP | | | |
| Kaolinite-supported iron oxide/PS/Vis LED | Rhodamine B (RhB) | <ul style="list-style-type: none"> The apparent rate constants of the processes of K-Fe/PS/Vis, PS/Vis and K-Fe/PS/dark are 1.57×10^{-2}, 6.60×10^{-3} and $4.10 \times 10^{-3} \text{ min}^{-1}$, respectively K-Fe showed high reusability and low level iron leading | [94] |
| Microwave (MW) irradiation/MnFe ₂ O ₄ | 4-nitrophenol | <ul style="list-style-type: none"> 20 mg L⁻¹ of 4-nitrophenol was degraded within 120 s [PMS] = 2.0 mM, [MnFe₂O₄] = 2.0 g L⁻¹ at pH 7 and MW output of 500 w MW irradiation creates a hotspot on the surface of the catalyst which enhances the PMS activation reaction | [80] |
| Ferro-ferric oxide coated on activated carbon (AC@Fe ₃ O ₄) | Tetracycline (TC) | <ul style="list-style-type: none"> pH = 3, 0.4 g L⁻¹ catalyst, 40 mM S₂O₈²⁻ were the optimal condition to remove 93.2%, 38.8% and 46.2% of TC, TOC, COD, respectively The efficiency did not change after five consecutive cycles of treatment SO₄^{•-} was the main radical involved in the degradation processes Iron leaching was <0.2 g L⁻¹ | [95] |
| TiO ₂ /UV-vis | Acid Orange 7 (AO7) | <ul style="list-style-type: none"> TiO₂/UV-vis/PMS was better than TiO₂/UV-vis/Ps system Humid acid had positive effect on AO7 degradation under TiO₂/UV-vis/PMS Total AO7 degradation within 100 min | [78] |
| α-sulfur/UV-vis | Rhodamine B | <ul style="list-style-type: none"> >99% rhodamine B [10 mg L⁻¹] removal in 60 min using [PMS] 0.3 g L⁻¹, [α-sulfur] 0.5 g L⁻¹ at 40 °C under 150 W visible light lamp | [96] |
| γ-MnO ₂ /rGO under ozonation | 4-nitrophenol | <ul style="list-style-type: none"> Completely degradation in 50 min Ozone decomposition was accelerated by PMS to form sulfate and hydroxyl radicals | [97] |
| Fe-Co/SBA-15 with ultrasonic irradiation | Orange II | <ul style="list-style-type: none"> >99% removal in 120 min Removal orange II rate was not effected by pH COD and TOC removal was 56.8% and 33.8% after 120 min, 80.1% and 53.3% after 24 h SO₄^{•-} was the dominating active species | [98] |

8. Conclusions and Implications for Future Applications

AOPs based on sulfate radical generation have attracted attention for applications in wastewater treatment and have been considered as a promising alternative treatment to remove recalcitrant organic compounds and traceable emerging contaminants. The advantages of sulfate radicals over traditional hydroxyl radicals are that they are more selective in the oxidation of target compounds and that they have a longer lifetime. Persulfate or peroxymonosulfate systems are often activated by alkali, heat, radiation, carbon based catalysts, and transition metals. The most used activation method is the use of transition metals; precisely, by Fe(II) or any other source of iron(II) such as zero valent iron. This activation is used more often because its performance can be enhanced by combining irradiation. Non-ferrous systems are also used, such as the use of Co, but the application is limited due to leaching of the metal into the environment. To overcome this problem, recent developments used persulfate or peroxymonosulfate activation by several carbon-based catalysts.

In summary, this work intended to highlight the major findings with regard to the application of sulphate radicals in the wastewater treatment for recovery and reuse. The results to date are very promising, and possible further applications could be in the treatment of leachates from irrigation waters, in order to be reused again for irrigation, which is an extremely important issue for arid areas, which rely heavily on agricultural activities.

Author Contributions: Monica Brienza and Ioannis A. Katsoyiannis contributed in writing the manuscript.

Conflicts of Interest: The authors declare no conflicts of interest.

References

1. Brienza, M.; Mahdi Ahmed, M.; Escande, A.; Plantard, G.; Scrano, L.; Chiron, S.; Bufo, S.A.; Goetz, V. Use of solar advanced oxidation processes for wastewater treatment: Follow up on degradation products, acute toxicity, genotoxicity and estrogenicity. *Chemosphere* **2016**, *148*, 473–480. [[CrossRef](#)] [[PubMed](#)]
2. Kong, L.; Kadokami, K.; Duong, H.T.; Chau, H.T.C. Screening of 1300 organic micro-pollutants in groundwater from Beijing and Tianjin, North China. *Chemosphere* **2016**, *165*, 221–230. [[CrossRef](#)] [[PubMed](#)]
3. Gómez, C.; Vicente, J.; Echavarri-Erasun, B.; Porte, C.; Lacorte, S. Occurrence of perfluorinated compounds in water, sediment and mussels from the Cantabrian Sea (North Spain). *Marine Pollut. Bull.* **2011**, *62*, 948–955. [[CrossRef](#)] [[PubMed](#)]
4. Babuponnusami, A.; Muthukumar, K. A review on Fenton and improvements to the Fenton processes for wastewater treatment. *J. Environ. Chem. Eng.* **2014**, *2*, 557–572. [[CrossRef](#)]
5. Glaze, W.H.; Kang, J.W.; Chapin, D.H. The chemistry of water treatment involving ozone, hydrogen peroxide and ultraviolet radiation. *Ozone Sci. Eng.* **1987**, *9*, 335–352. [[CrossRef](#)]
6. Katsoyiannis, I.A.; Canonica, S.; von Gunten, U. Efficiency and energy requirements for the transformation of organic micropollutants by ozone, O₃/H₂O₂ and UV/H₂O₂. *Water Res.* **2011**, *45*, 3811–3822. [[CrossRef](#)] [[PubMed](#)]
7. Bilińska, L.; Gmurek, M.; Ledakowicz, S. Comparison between industrial and simulated textile wastewater treatment by AOPs-Biodegradability, toxicity and cost assessment. *Chem. Eng. J.* **2016**, *306*, 550–559. [[CrossRef](#)]
8. Daghrir, R.; Drogui, P.; Robert, D. Modified TiO₂ for environmental photocatalytic applications: A review. *Ind. Eng. Chem. Res.* **2013**, *52*, 3581–3599. [[CrossRef](#)]
9. Matta, R.; Tlili, S.; Barbati, S. Removal of carbamazepine from urban wastewater by sulfate radical oxidation. *Environ. Chem. Lett.* **2011**, *9*, 347–353. [[CrossRef](#)]
10. Ahmed, M.; Barbati, S.; Doumenq, P.; Chiron, S. Sulfate radical anion oxidation of diclofenac and sulfaméthoxazole for water decontamination. *Chem. Eng. J.* **2012**, *197*, 440–447. [[CrossRef](#)]
11. Monteagudo, J.M.; Durán, A.; Latorre, J.; Expósito, A.J. Application of activated persulfate for removal of intermediates from antipyrine wastewater degradation refractory towards hydroxyl radical. *J. Hazard. Mater.* **2016**, *306*, 77–86. [[CrossRef](#)] [[PubMed](#)]

12. Ahmed, M.; Brienza, M.; Goetz, V.; Chiron, S. Solar photo-Fenton using peroxymonosulfate for organic micropollutants removal from domestic wastewater: Comparison with heterogeneous TiO₂ photocatalysis. *Chemosphere* **2014**, *117*, 256–261. [[CrossRef](#)] [[PubMed](#)]
13. Yang, Z.; Su, R.; Luo, S.; Spimmey, R.; Cai, M.; Xiao, R.; Wei, Z. Comparison of the reactivity of ibuprofen with sulfate and hydroxyl radicals: an experimental and theoretical study. *Sci. Total Environ.* **2017**, *590–591*, 751–760. [[CrossRef](#)] [[PubMed](#)]
14. Known, M.; Kim, S.; Yoon, Y.; Jung, Y.; Hwang, T.-M.; Lee, J.; Kang, J.-W. Comparative evaluation of ibuprofen removal by UV/H₂O₂ and UV/S₂O₈²⁻ processes for wastewater treatment. *Chem. Eng. J.* **2015**, *269*, 379–390.
15. Epold, I.; Trapido, M.; Dulova, N. Degradation of levofloxacin in aqueous solutions by Fenton, ferrous ion-activated persulfate and combined Fenton/persulfate systems. *Chem. Eng. J.* **2015**, *279*, 452–462. [[CrossRef](#)]
16. Gao, Y.; Zhang, Z.; Li, S.; Liu, L.; Yao, L.; Li, Y.; Zhang, H. Insights into the mechanism of heterogeneous activation of persulfate with a clay/iron-based catalyst under visible LED light irradiation. *Appl. Catal. B Environ.* **2016**, *185*, 22–30. [[CrossRef](#)]
17. Liu, H.; Bruton, T.A.; Li, W.; Buren, J.V.; Prasse, C.; Doyle, F.M.; Sedlak, D.L. Oxidation of benzene by persulfate in the presence of Fe(III)- and Mn(IV)-containing oxides: Stoichiometric efficiency and transformation products. *Environ. Sci. Technol.* **2016**, *50*, 890–898. [[CrossRef](#)] [[PubMed](#)]
18. Anipsitakis, G.P.; Dionysiou, D.D. Radical generation by the interaction of transition metals with common oxidants. *Environ. Sci. Technol.* **2004**, *38*, 3705–3712. [[CrossRef](#)] [[PubMed](#)]
19. Brienza, M.; Mahdi Ahmed, M.; Escande, A.; Plantard, G.; Scrano, L.; Chiron, S.; Bufo, S.A.; Goetz, V. Relevance of a photo-Fenton like technology based on peroxymonosulphate for 17β-estradiol removal from wastewater. *Chem. Eng. J.* **2014**, *257*, 191–199. [[CrossRef](#)]
20. Zhang, Q.; Chen, J.; Dai, C.; Zhang, Y.; Zhou, X. Degradation of carbamazepine and toxicity evaluation using the UV/persulfate process in aqueous solution. *J. Chem. Technol. Biotechnol.* **2014**, *90*, 701–708. [[CrossRef](#)]
21. Anipsitakis, G.P.; Tufano, T.P.; Dionysiou, D.D. Chemical and microbial decontamination of pool water using activated potassium peroxymonosulfate. *Water Res.* **2008**, *42*, 2899–2910. [[CrossRef](#)] [[PubMed](#)]
22. Deng, Y.; Zhao, R. Advanced oxidation processes (AOPs) in wastewater treatment. *Curr. Pollut. Rep.* **2015**, *1*, 167–176. [[CrossRef](#)]
23. Devi, P.; Das, U.; Dalai, A.K. In situ chemical oxidation: Principle and applications of peroxide and persulfate treatments in wastewater systems. *Sci. Total Environ.* **2016**, *571*, 643–657. [[CrossRef](#)] [[PubMed](#)]
24. Katsoyiannis, I.A.; Gkotsis, P.; Castellana, M.; Cartechini, F.; Zouboulis, A.I. Production of demineralized water for use in thermal power stations by advanced treatment of secondary wastewater effluent. *J. Environ. Manag.* **2017**, *190*, 132–139. [[CrossRef](#)] [[PubMed](#)]
25. Köck-Schulmeyer, M.; Villagrasa, M.; de Alda, M.L.; Céspedes-Sánchez, R.; Ventura, F.; Barceló, D. Occurrence and behavior of pesticides in wastewater treatment plants and their environmental impact. *Sci. Total Environ.* **2013**, *458–460*, 466–476. [[CrossRef](#)] [[PubMed](#)]
26. Zhang, Y.Q.; Huang, W.L.; Fennell, D.E. In situ chemical oxidation of aniline by persulfate with iron(II) activation at ambient temperature. *Chin. Chem. Lett.* **2010**, *21*, 911–913. [[CrossRef](#)]
27. Khan, J.A.; He, X.; Khan, H.M.; Shah, N.S.; Dionysiou, D.D. Oxidative degradation of atrazine in aqueous solution by UV/H₂O₂/Fe²⁺, UV/S₂O₈²⁻/Fe²⁺ and UV/HSO₅⁻/Fe²⁺ processes: A comparative study. *Chem. Eng. J.* **2013**, *281*, 376–383. [[CrossRef](#)]
28. Asha, T.T.; Gandhimathi, R.; Ramesh, S.T.; Nidheesh, P.V. Treatment of stabilized leachate by ferrous-activated persulfate oxidative system. *J. Hazard. Toxic Radioact. Waste* **2017**, *21*. [[CrossRef](#)]
29. Rastogi, A.; Al-Abed, S.R.; Dionysiou, D.D. Effect of inorganic, synthetic and naturally occurring chelating agents on Fe(II) mediated advanced oxidation of chlorophenols. *Water Res.* **2009**, *43*, 684–694. [[CrossRef](#)] [[PubMed](#)]
30. Rastogi, A.; Al-Abed, S.R.; Dionysiou, D.D. Sulfate radical-based ferrous-peroxymonosulfate oxidative system for PCBs degradation in aqueous and sediment systems. *Appl. Catal. B Environ.* **2009**, *85*, 171–179. [[CrossRef](#)]
31. Liang, C.; Bruell, C.J.; Marley, M.C.; Sperry, K.L. Persulfate oxidation for in situ remediation of TCE. II. Activated by chelated ferrous ion. *Chemosphere* **2004**, *55*, 1225–1233. [[CrossRef](#)] [[PubMed](#)]

32. Zhao, Y.S.; Sun, C.; Sun, J.Q.; Zhou, R. Kinetic modeling and efficiency of sulfate radical-based oxidation to remove p-nitroaniline from wastewater by persulfate/ Fe_3O_4 nanoparticles process. *Sep. Purif. Technol.* **2015**, *142*, 182–188. [[CrossRef](#)]
33. Dong, H.; He, Q.; Zeng, G.; Tang, L.; Zhang, L.; Xie, Y.; Zeng, Y.; Zhao, F. Degradation of trichloroethene by nanoscale zero-valent iron (nZVI) and nZVI activated persulfate in the absence and presence of EDTA. *Chem. Eng. J.* **2017**, *316*, 410–418. [[CrossRef](#)]
34. Oh, S.-Y.; Kim, H.-W.; Park, J.-M.; Park, H.-S.; Yoon, C. Oxidation of polyvinyl alcohol by persulfate activated whit heat, Fe^{2+} , and zero-valent iron. *J. Hazard. Mater.* **2009**, *168*, 346–351. [[CrossRef](#)] [[PubMed](#)]
35. Wang, Q.; Shao, Y.; Gao, N.; Chu, W.; Deng, J.; Shen, X.; Lu, X.; Zhu, Y.; Wei, X. Degradation of alachlor with zero-valent iron activating persulfate oxidation. *J. Taiwan Inst. Chem. Eng.* **2016**, *63*, 379–385. [[CrossRef](#)]
36. Wei, X.; Gao, N.; Li, C.; Deng, Y.; Zhou, S.; Li, L. Zero-valent iron (ZVI) activation of persulfate (PS) for oxidation of bentazon in water. *Chem. Eng. J.* **2016**, *285*, 660–670. [[CrossRef](#)]
37. Zeng, J.; Hu, L.; Tan, X.; He, C.; He, Z.; Pan, W.; Hou, Y.; Shu, D. Elimination of methyl mercaptan in ZVI-S₂O₈²⁻-system activated with in-situ generated ferrous ions from zero valent iron. *Catal. Today* **2017**, *281*, 520–526. [[CrossRef](#)]
38. Kambhu, A.; Gren, M.; Tang, W.; Comfort, S.; Harris, C.E. Remediating 1,4-dioxane-contaminated water with slow-release persulfate and zerovalent iron. *Chemosphere* **2017**, *175*, 170–177. [[CrossRef](#)] [[PubMed](#)]
39. Li, Y.; Zhang, Y.; Li, J.; Zheng, X. Enhanced removal of pentachlorophenol by a novel composite: Nanoscale zero valent iron immobilized on organobentonite. *Environ. Pollut.* **2011**, *159*, 3744–3749. [[CrossRef](#)] [[PubMed](#)]
40. Qiu, X.; Fang, Z.; Liang, B.; Gu, F.; Xu, Z. Degradation of decabromodiphenyl ether by nano zero valent iron immobilized in mesoporous silica microspheres. *J. Hazard. Mater.* **2011**, *193*, 70–81. [[CrossRef](#)] [[PubMed](#)]
41. Zhang, X.; Lin, S.; Chen, Z.L.; Megharaj, M.; Naidu, R. Kaolinite-supported nanoscale zero-valent iron for removal of Pb^{2+} from aqueous solution: Reactivity, characterization and mechanism. *Water Res.* **2011**, *45*, 3481–3488. [[CrossRef](#)] [[PubMed](#)]
42. Udayasoorian, C.; Ramalingam, P.; Jayabalakrishnan, R.M.; Vinoth Kumar, K. Carbon supported zero valent iron nanoparticles for treating PCP in pulp and paper effluent. *Res. J. Chem. Environ.* **2013**, *17*, 97–108.
43. Chen, Z.X.; Jin, X.Y.; Chen, Z.L.; Megharaj, M.; Naidu, R. Removal of methyl orange from aqueous solution using bentonite-supported nanoscale zero-valent iron. *J. Colloid Interface Sci.* **2011**, *363*, 601–607. [[CrossRef](#)] [[PubMed](#)]
44. Diao, Z.-H.; Xu, X.-R.; Jiang, D.; Kong, L.-J.; Sun, Y.-X.; hu, Y.-X.; Hao, Q.-W.; Chen, H. Bentonite-supported nanoscale zero-valent iron/persulfate system for the simultaneous removal of Cr(VI) and phenol from aqueous solutions. *Chem. Eng. J.* **2016**, *302*, 213–222. [[CrossRef](#)]
45. Liang, C.; Liang, C.P.; Chen, C.C. pH dependence of persulfate activation by EDTA/Fe (III) for defradation of trichloroethylene. *J. Contam. Hydrol.* **2009**, *106*, 173–182. [[CrossRef](#)] [[PubMed](#)]
46. Liang, C.J.; Lin, Y.T.; Shih, W.H. Treatment of trichloroethylene by adsorption and persulfate oxidation in batch studies. *Ind. Eng. Chem. Res.* **2009**, *48*, 8373–8380. [[CrossRef](#)]
47. Dulova, N.; Kattel, E.; Trapido, M. Degradation of naproxen by ferrous ion-activated hydrogen proxide, persulfate and combined hydrogen peroxide/persulfate processes: The effect of citric acid addition. *Chem. Eng. J.* **2017**, *318*, 254–263. [[CrossRef](#)]
48. Katsoyiannis, I.A.; Ruettimann, T.; Hug, S.J. pH dependence of Fenton reagent generation and As(III) oxidation and removal by corrosion of zero valent iron in aerated water. *Environ. Sci. Technol.* **2008**, *42*, 7424–7430. [[CrossRef](#)] [[PubMed](#)]
49. Funai, D.H.; Didier, F.; Giménez, J.; Esplugas, S.; Marco, P.; Machulek Junior, A. Photo-Fenton treatment of valproate under UVC, UVA and simulated solar radiation. *J. Hazard. Mater.* **2017**, *323*, 537–549. [[CrossRef](#)] [[PubMed](#)]
50. Ahmadi, M.; Mohseni, M.; Vahabzadeh, F. Study on trend of biodegradability of phenolic compounds during photo-fenton advanced oxidation process. *Iran. J. Chem. Eng.* **2008**, *5*, 23–32.
51. Spuhler, D.; Rengifo-Herrera, J.; Pulgarin, C. The effect of Fe^{2+} , Fe^{3+} , H_2O_2 and the photo-Fenton reagent at near neutral pH on the solar disinfection (SODIS) at low temperatures of water containing *Escherichia coli* K12. *Appl. Catal. B* **2010**, *96*, 126–141. [[CrossRef](#)]
52. Oller, I.; Malato, S.; Sánchez-Pérez, J.A. Combination of advanced oxidation processes and biological treatment for wastewater decontamination—A review. *Sci. Total Environ.* **2011**, *409*, 4114–4166. [[CrossRef](#)] [[PubMed](#)]

53. Bernabeua, A.; Verchera, R.F.; Santos-Juanesa, L.; Simónb, P.J.; Lardínb, C.; Martínezc, M.A.; Vicentec, J.A.; Gonzálezc, R.; Llosác, C.; Arquesa, A.; et al. Solar photocatalysis as tertiary treatment to remove emerging pollutants from wastewater treatment plant effluents. *Catal. Today* **2011**, *161*, 235–240. [[CrossRef](#)]
54. Klammerth, N.; Malato, S.; Maldonado, M.I.; Agüera, A.; Fernandez-Alba, A.R. Application of Photo-Fenton as a tertiary treatment of emerging contaminants in municipal wastewater. *Environ. Sci. Technol.* **2010**, *44*, 1792–1798. [[CrossRef](#)] [[PubMed](#)]
55. Prieto-Rodríguez, L.; Spasiano, D.; Oller, I.; Fernández-Calderero, I.; Agüera, A.; Malato, S. Solar photo-Fenton optimization for the treatment of MWTP effluents containing emerging contaminants. *Catal. Today* **2013**, *209*, 188–194. [[CrossRef](#)]
56. Leshuk, T.; Wong, T.; Linley, S.; Peru, K.M.; Headley, J.V.; Gu, F. Solar photocatalytic degradation of naphthenic acids in oil sands process-effected water. *Chemosphere* **2016**, *144*, 1854–1861. [[CrossRef](#)] [[PubMed](#)]
57. Malato, S.; Maldonado, M.I.; Fernández-Ibáñez, P.; Oller, I.; Polo, I.; Sánchez-Moreno, R. Decontamination and disinfection of water by solar photocatalysis: The pilot plants of the Plataforma Solar de Almeria. *Mater. Sci. Semicond. Process.* **2016**, *42*, 15–23. [[CrossRef](#)]
58. Dhatshanamurthi, P.; Shanthi, M.; Swaminathan, M. An efficient pilot scale solar treatment method for dye industry effluent using nano-ZnO. *J. Water Processes Eng.* **2017**, *16*, 28–34. [[CrossRef](#)]
59. Khandarkhaeva, M.; Batoeva, A.; Aseev, D.; Sizykh, M.; Tsydenova, O. Oxidation of atrazine in aqueous media by solar-enhanced Fenton like process involving persulfate and ferrous ion. *Ecotoxicol. Environ. Saf.* **2017**, *137*, 35–41. [[CrossRef](#)] [[PubMed](#)]
60. Lin, C.-C.; Wu, M.-S. Degradation of ciprofloxacin by UV/S2O8²⁻-process in a large photoreactor. *J. Photochem. Photobiol. A* **2014**, *285*, 1–6. [[CrossRef](#)]
61. Anipsitakis, G.P.; Stathatos, E.; Dionysiou, D.D. Heterogeneous activation of Ozone using Co₃O₄. *J. Phys. Chem. B* **2005**, *109*, 13052–13055. [[CrossRef](#)] [[PubMed](#)]
62. Hu, P.; Long, M. Cobalt-catalyzed sulfate radical-based advanced oxidation: A review on heterogeneous catalysts and applications. *Appl. Catal. B Environ.* **2016**, *181*, 103–117. [[CrossRef](#)]
63. Zhang, J.; Chen, M.; And Zhu, L. Activation of persulfate by Co₃O₄ nanoparticles for orange G degradation. *RSC Adv.* **2016**, *5*, 758–768. [[CrossRef](#)]
64. Deng, J.; Shao, Y.; Gao, N.; Tan, C.; Zhou, S.; Hu, X. CoFe₂O₄ magnetic nanoparticles as highly active heterogeneous catalyst of oxone for degradation of diclofenac in water. *J. Hazard. Mater.* **2013**, *262*, 836–844. [[CrossRef](#)] [[PubMed](#)]
65. Shukla, P.; Sun, H.; Wang, S.; Ang, H.M.; Tade, M.O. Co-SBA-15 for heterogeneous oxidation of phenol with sulphate radical for wastewater treatment. *Catal. Today* **2011**, *175*, 380–385. [[CrossRef](#)]
66. Shi, P.; Su, R.; Wan, F.; Zhu, M.; Li, D.; Xu, S. Co₃O₄ nanocrystals on graphene oxide as a synergistic catalyst for degradation of Orange II in water by advanced oxidation technology based on sulfate radicals. *Appl. Catal. B Environ.* **2011**, *123–124*, 265–272. [[CrossRef](#)]
67. Saputra, E.; Muhammad, S.; Sun, H.; Ang, H.; Tade, M.O.; Wang, S. Manganese oxides at different oxidation states for heterogeneous activation of peroxydisulfate for phenol degradation in aqueous solutions. *Appl. Catal. B Environ.* **2013**, *142–143*, 729–735. [[CrossRef](#)]
68. Liu, C.S.; Shih, K.; Sun, C.X.; Wang, F. Oxidative degradation of propachlor by ferrous and copper ion activated persulfate. *Sci. Total Environ.* **2012**, *416*, 507–512. [[CrossRef](#)] [[PubMed](#)]
69. Fang, G.; Wu, W.; Liu, C.; Dionysiou, D.D.; Deng, Y.; Zhou, D. Activation of persulfate with vanadium species for PCBs degradation: A mechanistic study. *Appl. Catal. B Environ.* **2017**, *202*, 1–11. [[CrossRef](#)]
70. Duan, X.; Su, C.; Zhou, L.; Sun, H.; Suvorova, A.; Odedairo, T.; Zhu, Z.; Shao, Z.; Wang, S. Surface controlled generation of reactive radicals from persulfate by photocatalysis on nanodiamonds. *Appl. Catal. B Environ.* **2016**, *194*, 7–15. [[CrossRef](#)]
71. Indrawirawan, S.; Sun, H.; Duan, X.; Wang, S. Nanocarbons in different structural dimensions (0–3D) for phenol adsorption and metal-free catalytic oxidation. *Appl. Catal. B* **2015**, *179*, 352–362. [[CrossRef](#)]
72. Kimura, M.; Miyamoto, I. Discovery of the activated carbon radical AC⁺ and the novel oxidation reactions comprising the AC/AC⁺ cycle as a catalyst in an aqueous solution. *Bull. Chem. Soc. Jpn.* **1994**, *67*, 2357–2360. [[CrossRef](#)]
73. Muhammad, S.; Shukla, P.R.; Tade, M.O.; Wang, S. Heterogeneous activation of peroxydisulfate by supported ruthenium catalysts for phenol degradation in water. *J. Hazard. Mater.* **2012**, *215–216*, 183–190. [[CrossRef](#)] [[PubMed](#)]

74. Yang, S.; Xiao, T.; Zhang, J.; Chen, Y.; Li, L. Activated carbon fiber as heterogeneous catalyst of peroxymonosulfate activation for efficient degradation of Acid Orange 7 in aqueous solution. *Sep. Purif. Technol.* **2015**, *143*, 19–26. [[CrossRef](#)]
75. Zhang, J.; Shao, X.; Shi, C.; Yang, S. Decolorization of acid Orange 7 with peroxymonosulfate oxidation catalyzed by granular activated carbon. *Chem. Eng. J.* **2013**, *232*, 259–265. [[CrossRef](#)]
76. Peng, W.; Liu, S.; Sun, H.; Yao, Y.; Zhic, L.; Wang, S. Synthesis of porous reduced graphene oxide as metal-free carbon for adsorption and catalytic oxidation of organics in water. *J. Mater. Chem. A* **2013**, *1*, 5854–5859. [[CrossRef](#)]
77. Duan, X.; Ao, Z.; Zhou, L.; Sun, H.; Wang, G.; Wang, S. Occurrence of radical and nonradical pathways from carbocatalysts for aqueous and non aqueous catalytic oxidation. *Appl. Catal. B Environ.* **2016**, *188*, 98–105. [[CrossRef](#)]
78. Chen, X.; Wang, W.; Xiao, H.; Hong, C.; Zhu, F.; Yao, Y.; Xue, Z. Accelerated TiO₂ photocatalytic degradation of Acid Orange 7 under visible light mediated by peroxymonosulfate. *Chem. Eng. J.* **2012**, *193–194*, 290–295. [[CrossRef](#)]
79. Kuriechen, S.K.; Murugesan, S.; Raj, S.P.; Maruthamuthu, P. Visible light assisted photocatalytic mineralization of Reactive Red 180 using colloidal TiO₂ and oxone. *Chem. Eng. J.* **2011**, *174*, 530–538. [[CrossRef](#)]
80. Pang, Y.; Lei, H. Degradation of p-nitrophenol through microwave-assisted heterogeneous activation of peroxymonosulfate by manganese ferrite. *Chem. Eng. J.* **2016**, *287*, 585–592. [[CrossRef](#)]
81. Zhao, L.; Ji, Y.; Kong, D.; Lu, J.; Zhou, Q.; Yin, X. Simultaneous removal of bisphenol A and phosphate in zero-valent iron activated persulfate oxidation processes. *Chem. Eng. J.* **2016**, *303*, 458–466. [[CrossRef](#)]
82. Li, H.; Wan, J.; Ma, Y.; Wang, Y. Reaction pathway and oxidation mechanisms of dibutyl phthalate by persulfate activated with zero-valent iron. *Sci. Total Environ.* **2016**, *303*, 458–466.
83. Qin, W.; Fang, G.; Wang, Y.; Wu, T.; Zhu, C.; Zhou, D. Efficient transformation of DDT by peroxymonosulfate activated by cobalt in aqueous systems: Kinetics, products, and reactive species identification. *Chemosphere* **2016**, *148*, 68–76. [[CrossRef](#)] [[PubMed](#)]
84. Li, H.; Wan, J.; Ma, Y.; Wang, Y.; Chen, X.; Guan, Z. Degradation of refractory dibutyl phthalate by peroxymonosulfate activated with novel catalysts cobalt metal-organic frameworks: Mechanism, performance, and stability. *J. Hazard. Mater.* **2016**, *318*, 154–163. [[CrossRef](#)] [[PubMed](#)]
85. Liang, H.-Y.; Zhang, Y.-Q.; Huang, S.-B.; Hussain, I. Oxidative degradation of p-chloroaniline by copper oxidate activated persulfate. *Chem. Eng. J.* **2013**, *218*, 348–391. [[CrossRef](#)]
86. Ji, Q.; Li, J.; Xiong, Z.; Lai, B. Enhanced reactivity of microscale Fe/Cu bimetallic particles (mFe/Cu) with persulfate (PS) for p-nitrophenol (PNP) removal in aqueous solution. *Chemosphere* **2017**, *172*, 10–20. [[CrossRef](#)] [[PubMed](#)]
87. Li, H.; Guo, J.; Yang, L.; Lan, Y. Degradation of methyl orange by sodium persulfate activated with zero-valent zinc. *Sep. Purif. Technol.* **2014**, *132*, 168–173. [[CrossRef](#)]
88. Liang, S.X.; Jia, Z.; Zhang, W.C.; Wang, W.M.; Zhang, L.C. Rapid malachite green degradation using Fe_{73.5}Si_{13.5}B₉Cu₁Nb₃ metallic glass for activation of persulfate under UV-Vis light. *Mater. Des.* **2017**, *119*, 244–253. [[CrossRef](#)]
89. Jiang, M.; Lu, J.; Ji, Y.; Kong, D. Bicarbonate-activated persulfate oxidation of acetaminophen. *Water Res.* **2017**, *116*, 324–331. [[CrossRef](#)] [[PubMed](#)]
90. Guo, Y.; Zeng, Z.; Li, Y.; Huang, Z.; Yang, J. Catalytic oxidation of 4-chlorophenol on in-situ sulphur-doped activated carbon with sulphate radicals. *Sep. Purif. Technol.* **2017**, *179*, 257–264. [[CrossRef](#)]
91. Lee, H.; Lee, H.-J.; Jeong, J.; Lee, J.; Park, N.-B.; Lee, C. Activation of persulfates by carbon nanotubes: Oxidation of organic compounds by nonradical mechanisms. *Chem. Eng. J.* **2015**, *266*, 28–33. [[CrossRef](#)]
92. Sun, H.; Kwan, C.; Suvorova, A.; Ang, H.M.; Tadé, M.O.; Wang, S. Catalytic oxidation of organic pollutants on pristine and surface nitrogen-modified carbon nanotubes with sulfate radicals. *Appl. Catal. B Environ.* **2014**, *154–155*, 134–141. [[CrossRef](#)]
93. Kang, J.; Duan, X.; Zhou, L.; Sun, H.; Tadé, M.O.; Wang, S. Carbocatalytic activation of persulfate for removal of antibiotics in water solutions. *Chem. Eng. J.* **2016**, *288*, 399–405. [[CrossRef](#)]
94. Duan, X.; Sun, H.; Kang, J.; Wang, Y.; Indrawirawan, S.; Wang, S. Insights into heterogeneous catalysis of persulfate activation on dimensional-structured nanocarbons. *ACS Catal.* **2015**, *5*, 4629–4636. [[CrossRef](#)]

95. Jafari, A.J.; Kakavandi, B.; Jaafarzadeh, N.; Kalantary, R.R.; Ahmadi, M.; Barbaei, A.A. Fenton-like catalytic oxidation of tetracycline by AC@Fe₃O₄ as a heterogeneous persulfate activator: adsorption and degradation studies. *J. Ind. Eng. Chem.* **2017**, *45*, 323–333. [[CrossRef](#)]
96. Andrew Lin, K.Y.; Zhang, Z.-Y. α -Sulfur as a metal-free catalyst to active peroxymonosulfate under visible light irradiation for decolorization. *RSC Adv.* **2016**, *6*, 15027–15034. [[CrossRef](#)]
97. Wang, Y.; Xie, Y.; Sun, H.; Xiao, J.; Cao, H.; Wang, S. 2D/2D nano-hybrids of γ -MnO₂ on reduced graphene oxide for catalytic ozonation and coupling peroxymonosulfate activation. *J. Hazard. Mater.* **2016**, *301*, 56–64. [[CrossRef](#)] [[PubMed](#)]
98. Cai, C.; Zhang, H.; Zhong, X.; Hou, L. Ultrasound enhanced heterogeneous activation of peroxymonosulfate by a bimetallic Fe-Co/SBA-15 catalyst for degradation of Orange II in water. *J. Hazard. Mater.* **2015**, *283*, 70–79. [[CrossRef](#)] [[PubMed](#)]



© 2017 by the authors. Licensee MDPI, Basel, Switzerland. This article is an open access article distributed under the terms and conditions of the Creative Commons Attribution (CC BY) license (<http://creativecommons.org/licenses/by/4.0/>).